


Bioinformatics-Guided Discovery of miRNAs Involved in Apoptosis Modulated by Parthenolide Combined with Vincristine in The NALM6 Cell Line

Atefeh Bahmei, M.Sc.¹, Sepideh Namdari, M.Sc.², Mohammad Yaghoubzad-Maleki, M.Sc.³, Ali Emami, M.Sc.⁴,
Reza Ranjbaran, Ph.D.², Gholamhossein Tamaddon, Ph.D.^{1,2*} 

1. Division of Hematology and Blood bank, Department of Medical Laboratory Sciences, School of Paramedical Sciences, Shiraz University of Medical Sciences, Shiraz, Iran

2. Diagnostic Laboratory Sciences and Technology Research Center, School of Paramedical Sciences, Shiraz University of Medical Sciences, Shiraz, Iran

3. Division of Biochemistry, Department of Animal Biology, Faculty of Natural Sciences, University of Tabriz, Iran

4. Department of Biochemistry and Molecular Medicine, University of Montreal, Montreal, Canada

Abstract

Objective: Acute lymphoblastic leukemia (ALL) is a highly heterogeneous leukemia. Despite the current improvement in conventional chemotherapy and high survival rates, the outcomes remain challenging. Sesquiterpen extracted from the *Tanacetum parthenium*, parthenolide, is a potential anticancer agent that can modulate the expression of miRNAs and induce apoptosis. The objective of this study was to investigate the effect of parthenolide in combination with vincristine and alone on the apoptosis rate and expression of miR-125b-5p, miR-181b-5p, and miR-17-5p in the NALM6 cell line.

Materials and Methods: In this experimental study, cell viability and metabolic activity were determined through MTT assay and PI staining. Flow cytometry was applied to evaluate the rate of apoptosis. The expression of miRNAs was assessed using real-time polymerase chain reaction. Bioinformatic analyses, including Cytoscape, RNAhybrid, and signaling pathway analysis were employed to investigate the association of miR-17-5p, miR-181b-5p and miR-125b-5p with apoptosis. Further, molecular docking served to validate the modulation of these miRNAs by parthenolide and vincristine treatment.

Results: The MTT assay indicated that 7.7 μ M of parthenolide decreased the metabolic activity to 50% after 48 hours. PI staining analysis indicated that at concentrations below the half maximal inhibitory concentration, parthenolide caused 50% cell death. Flow cytometric analysis indicated that parthenolide (1.925 μ M) in combination with vincristine (1.2 nM) induced apoptosis in 83.2% of the cells. Real-time quantitative reverse transcription polymerase chain reaction (qRT-PCR) analysis showed significant changes in the expression levels of miR-17-5p, miR-125b-5p, and miR-181b-5p. Moreover, the combination therapy downregulated the expression of miRNAs significantly. This was consistent with our bioinformatic analysis demonstrating that the studied miRNAs are regulators of apoptosis. Finally, molecular docking validated the modulation of the miRNAs by parthenolide and vincristine.

Conclusion: Parthenolide in combination with vincristine triggers apoptosis at a high rate in the NALM6 cell line. Moreover, this combination therapy can decrease the expression of miR-17-5p, miR-181b-5p, and miR-125b-5p.

Keywords: Apoptosis, B-Acute Lymphoblastic Leukemia, Bioinformatics, miRNAs, Parthenolide

Citation: Bahmei A, Namdari S, Yaghoubzad-Maleki M, Emami A, Ranjbaran R, Tamaddon Gh. Bioinformatics-guided discovery of mirnas involved in apoptosis modulated by parthenolide combined with vincristine in the nalm6 cell line. Cell J. 2024; 26(2): 139-149. doi: 10.22074/CELLJ.2024.2013673.1428
This open-access article has been published under the terms of the Creative Commons Attribution Non-Commercial 3.0 (CC BY-NC 3.0).

Introduction

Acute lymphoblastic leukemia (ALL) is a highly heterogeneous leukemia typically classified as B cell ALL (B-ALL) or T cell ALL (T-ALL). B-ALL accounts for approximately 85% of the cases (1). ALL is the most common pediatric cancer, representing 25% of cancer diagnoses in children (2). However, B-ALL can affect both children and adults (3). Despite the current high survival rates, improving conventional chemotherapy outcomes remains challenging, as the risk of relapse or refractory leukemia remains high (4). Therefore, it is crucial to explore new treatment methods and identify

therapeutic biomarkers to enhance the quality of life and prognosis for ALL patients.

NALM6 is a B cell precursor leukemia cell line derived from the peripheral blood of a patient with ALL. These cells are commonly used as a model for studying tumor growth, metastasis, B-cell differentiation, and evaluating the effects of various drugs or therapies in animals (5).

MicroRNAs (miRNAs) are small, single-stranded, non-coding RNA molecules containing 21 to 23 nucleotides. They are involved in RNA silencing and post-transcriptional regulation of gene expression.

Received: 16/October/2023, Revised: 10/January/2024, Accepted: 21/January/2024

*Corresponding Address: P.O.Box: 7134814336, Division of Hematology and Blood bank, Department of Medical Laboratory Sciences, School of Paramedical Sciences, Shiraz university of medical Sciences, Shiraz, Iran
Email: tamaddon@sums.ac.ir



Royan Institute
Cell Journal
(Yakhteh)

MiRNAs can bind to complementary sequences in mRNA molecules, leading to gene silencing through processes such as cleavage of mRNA strands or destabilization of mRNA (6). They play critical roles in different pathways, especially apoptosis, and are also implicated in various pathological conditions, including ALL (7). The miRNAs studied in B-ALL can play tumorigenic or tumor suppressor roles. The miR-181 family, which includes miR-181b, is described as a regulator of early B cell development. On the other hand, miR-125b has a vital role in hematopoietic differentiation in two directions of myeloid or lymphoid population based on its expression level and the time point when it is expressed. Also, the overexpression of miR-125b in embryonic hematopoietic cells could induce B-ALL *in vivo*. Furthermore, mice deficient in miR-17-92 cluster have B-cell maturation arrest in early stages, highlighting the significance of miR-17-92 cluster in B-cell lymphopoiesis. Recently, it has been demonstrated that these miRNAs are upregulated in B-ALL and target different factors including BTG2, PTEN, P53, BCL-2, and Bak1, resulting in reduced apoptosis (8, 9). Moreover, the downregulation of miR-17-5p, miR-181b-5p, and miR-125b-5p in the context of apoptosis signaling is significant (10, 11).

Apoptosis has been studied widely and is characterized by the activation of caspases, which are proteases that degrade cellular proteins. This process is regulated by two main signaling pathways: the intrinsic (mitochondrial) and the extrinsic (death receptor-mediated) pathways. The intrinsic pathway involves the release of cytochrome C from the mitochondria into the cytosol, leading to caspase activation and eventually cell death. On the other hand, the extrinsic pathway involves the activation of death receptors on the cell surface, which recruits adaptor molecules and forms the death-inducing signaling complex. This complex initiates a cascade of events similar to the intrinsic pathway, leading to caspase activation. MiRNAs can regulate apoptosis by targeting genes involved in both intrinsic and extrinsic pathways (12).

Parthenolide is a component of *Tanacetum parthenium* that has been found to influence key biological processes in cells, especially apoptosis. Parthenolide was traditionally used to treat migraine, fever, and rheumatoid arthritis but recent studies have found it to be effective in treating various cancers (13, 14). Also, previous studies have focused on the effect of parthenolide on apoptosis in several cancers. However, few studies have investigated its association with miRNAs. Therefore, the main goal of this study was to examine whether there would be a synergistic effect between parthenolide and vincristine, and how this combination could alter the expression of miR-17-5p, miR-125b-5p, and miR-181b-5p in the NALM6 cell line.

Materials and Methods

This experimental study was approved by the Ethics Committee of Shiraz University of Medical Sciences (IR.SUMS.REC.1401.173). All tests were conducted

in Diagnostic Laboratory Sciences and Technology Research Center, School of Paramedical Sciences, Shiraz University of Medical Sciences, Shiraz, Iran. The NALM6 cell line was kindly provided by Dr. Majid Safa (Iran University of Medical Sciences, Tehran, Iran) which was previously purchased from ATCC. All materials and reagents used for cell culture were purchased from Gibco Life Technologies (Waltham, MA) and Sigma-Aldrich (Munich, Germany). Parthenolide (5.0 mg) was acquired from Sigma-Aldrich (Munich, Germany) and was prepared using dimethyl sulfoxide (DMSO).

Cell culture

NALM6 cells (CRL-3273™) were cultured under standard conditions at 37°C in a humidified 5% CO₂ incubator. RPMI-1640 medium (ATCC® 30-2001™) supplemented with 10% fetal bovine serum (FBS, ATCC® 30-2020™), 100 U/ml penicillin-streptomycin, and 2 mM glutamine was used for cell culture. ATCC's protocol (5) was followed for the culture method. Trypan blue staining was performed for the examination of cell viability.

Metabolic activity assessment

To examine the potential impact of parthenolide on metabolic activity, NALM6 cells were seeded into 96-well culture plates at a density of 2×10^4 cells/well in 200 µL of growth medium and treated with varying concentrations of parthenolide and vincristine (as positive controls). The concentrations ranged from 1 µM to 32 µM for parthenolide, and 0.5 nM to 5 nM for vincristine. Following a 48-hour incubation, MTT assay was conducted using 20 µL of sterile 3-(4,5-dimethylthiazol-2-yl)-2,5-diphenyl-tetrazolium bromide (MTT, Sigma-Aldrich, Germany, Darmstadt). Following the removal of the MTT solution, 150 µL DMSO was added to each well to dissolve the formazan crystals. Spectrometric absorbance at 570 nm was measured using a BioTek ELx800 microplate photometer (BioTek ELx800, SN211805; BioTek, Winooski, VT). The half maximal inhibitory concentration (IC₅₀) values were determined by comparing the experimental cells with their respective controls. Mean values were calculated from triplicate cultures.

Propidium iodide staining

To further investigate the inhibitory effects of parthenolide and vincristine on cell growth, propidium iodide (PI) was utilized as a viability stain (MabTags, Germany). A total of 1×10^5 cells were suspended in 800 µL of fresh media and plated in each well of a 24-well microtiter plate. The cells were then incubated overnight. Subsequently, parthenolide and vincristine were added at 0, 7.7, 3.85, 1.925, 0.96 µM for parthenolide and 0, 3.21, 1.6, 0.8, 0.4 nM for vincristine. After 48 hours, the cells were harvested and washed twice with cold phosphate-buffered saline (PBS). A solution containing 1×10^5 cells (100 µL) was mixed with 5 µL of PI following

the manufacturer's instructions. The mixed solution was incubated at room temperature in the absence of light for 15 minutes. The reaction of PI binding was analyzed quantitatively using a FACScalibur flow cytometer (BD Biosciences) and FlowJo software (TreeStar LLC).

Apoptosis assay

In each well of a 24-well microtiter plate, 1×10^5 cells were suspended in 800 μ l of fresh medium and incubated overnight. Subsequently, parthenolide, vincristine, and a combination of both were added at the 2.8, 1.925 μ M for parthenolide and 1.2, 0.8 nM for vincristine. After 48 hours, the cells were harvested and washed twice with cold PBS. The washed cells were then resuspended in 90 μ l of diluted (1x) Annexin-V binding buffer at a concentration of 1×10^5 cells/ml. Next, 5 μ l of annexin V-FITC solution, containing the cells, and 5 μ l of PI were mixed (MabTag's Annexin-V Apoptosis Detection Kit, Germany) following the manufacturer's instructions. The mixed solution was incubated at 25°C in the absence of light for 15 minutes. Subsequently, 400 μ l Annexin-V binding buffer (1x) was added to each tube. Centrifugation at 400 g for 5 minutes was performed. Analysis was conducted using a FACScalibur flow cytometer (BD Biosciences) and FlowJo software (TreeStar LLC).

RNA extraction

After 48 hours of treatment with parthenolide extract, vincristine, and the combination of both, total RNA was isolated using TRIzol reagent (Thermo Fisher Scientific). The quality of the extracted RNA was evaluated based on the 260/280 and 260/230 ratios using a NanoDrop spectrophotometer (Thermo Scientific NanoDrop2000, Finland).

cDNA synthesis

For this study, reverse transcriptase (RT) microRNA PCR kit (Pars genome, Iran) was utilized to synthesize DNA. For the cDNA synthesis process, 2 μ g of total RNA was used. Subsequently, the samples were incubated at 45°C for 60 minutes. Finally, the samples were heated at 85°C for 5 minutes to inactivate the RT enzyme.

MiR-17-5p, miR-125b-5p, and miR-181b-5p real-time quantitative reverse transcription polymerase chain reaction (qRT-PCR) assays were performed with ABI 7500 real-time PCR equipment (Applied Biosystems, USA). SYBR Green Master Mix and specific primers were purchased from Pars Gene (Pars genome, Iran). To normalize the miRNA expression data, 5S rRNA was chosen as the housekeeping gene.

Real-time polymerase chain reaction

The qRT-PCR assay was performed with the following conditions: initial denaturation at 95°C for 15 minutes, followed by 40 cycles of amplification consisting of 95°C for 30 seconds, 62°C for 30 seconds, and 72°C for 30 seconds. The comparative CT technique was utilized to

calculate the relative fold changes in miRNA expression for each sample, using the formula $RQ = 2^{-\Delta\Delta Ct}$.

Bioinformatics analysis

Network creation

First, the targets of microRNAs were downloaded using the miRDB database and imported into Cytoscape to predict the miRNA and mRNA Model network. Apoptosis-related genes have been identified. RNAhybrid was used to predict miRNA binding site and potential mRNA targets related to apoptosis regulation.

Cell signaling pathway enrichment

Data extracted from miRDB were prepared in an Excel file with two columns and a compatible format. The prepared data were uploaded to a bioinformatics platform (<https://www.bioinformatics.com.cn/>). On the Go pathway enrichment analysis platform, the data were copied and pasted into the input frame, and parameters were selected for analysis, such as miRNA target prediction and signaling pathway enrichment with a $P < 0.05$. After submitting the analysis, the results were downloaded from the bioinformatics platform. The downloaded results were uploaded to RStudio (<https://rstudio.com/>). The ggplot2 package in R was used to create graphical representations of the miRNA predictions.

Molecular docking

We performed molecular docking to validate the direct binding and binding affinity of miRNA-ligand interactions and to analyze the binding potential and nucleotide regions involved in the binding conformation. The 2D formats of ligands were downloaded as a spline font database file from the PubChem chemical database. To optimize the structures, the SDF formats of the ligands were subjected to energy minimization and partial molecular dynamics by Chem3D 17.1 software, to get the best conformation. Finally, the structural files of the ligands were saved as PDB files. To make the structures of miRNA molecules, their sequences were taken from the RNACentral database, and the structures of miRNAs were created by Avogadro software v1.2.0 and saved as a PDB file. Lastly, molecular docking was carried out using AutoDock Vina. Polar hydrogen atoms and Gasteiger charges were added to the targets and ligand molecules and miRNAs were converted to pdbqt files and saved separately. The size of the grid box was chosen according to the size of the miRNAs to cover the entire molecule. The docking output poses were selected based on the affinity binding. The bases involved in binding with ligands were displayed by biovia discovery studio v2021 and the positions of miRNAs and ligands relative to each other were checked by UCSF-Chimera v1.16. Next, to check the binding affinity of the ligands in the presence of each other, the complexes of all the ligands with miRNAs were made by the biovia discovery studio v2021, and the complexes were again subjected to molecular docking with AutoDock Vina in the same way

as before (15, 16).

Statistical analysis

Statistical analysis was conducted using GraphPad Prism (version 8.4.3, GraphPad Software, Inc. USA). The data were analyzed using One-way ANOVA followed by Tukey's test for multiple comparisons with a statistical significance of $P < 0.05$.

Results

Effects of parthenolide and vincristine on the metabolic activity of NALM6 cells

The MTT assay showed that both parthenolide and vincristine had dose-dependent inhibitory effects on NALM6 cell line. Compared to controls, parthenolide reduced metabolic activity from 98.2 to 94.08%, and from 77.8 to 29.5% after 48 hours of treatment in NALM6 cells, respectively (Fig.1A). Similarly, vincristine reduced the metabolic activity of NALM6 cells from 75.1 to 69.2%,

and from 54.6 to 32.4% respectively. The concentration of parthenolide required to inhibit NALM6 metabolic activity by 50% (IC_{50}) at 48 hours was 7.7 μ M. The IC_{50} value of vincristine for NALM6 cells was 3.21 nM.

Effects of parthenolide and vincristine on the cell viability of NALM6 cell line using PI-staining

To further determine the anti-cancer activity of parthenolide and vincristine on human NALM6 cells, the cells were treated with 0, 7.7, 3.85, 1.925, and 0.96 μ M parthenolide for 48 hours. The viability of the cells was measured using PI staining and flow cytometry. After treatment with parthenolide and vincristine, the viability of NALM6 cells was significantly decreased in a dose-dependent manner. The cell death rates were 6.278, 96.95, 87.50, 33.55, and 13.98% after treatment with parthenolide for 48 h (Fig.1B). Also, the rates were 6.495 \pm 1.01, 92.78 \pm 1.890, 90.61 \pm 2.017, 56.08 \pm 3.271, and 16.43 \pm 1.127 % after treatment with 0, 3.21, 1.6, 0.8, and 0.4 nm of vincristine (Fig.1C).

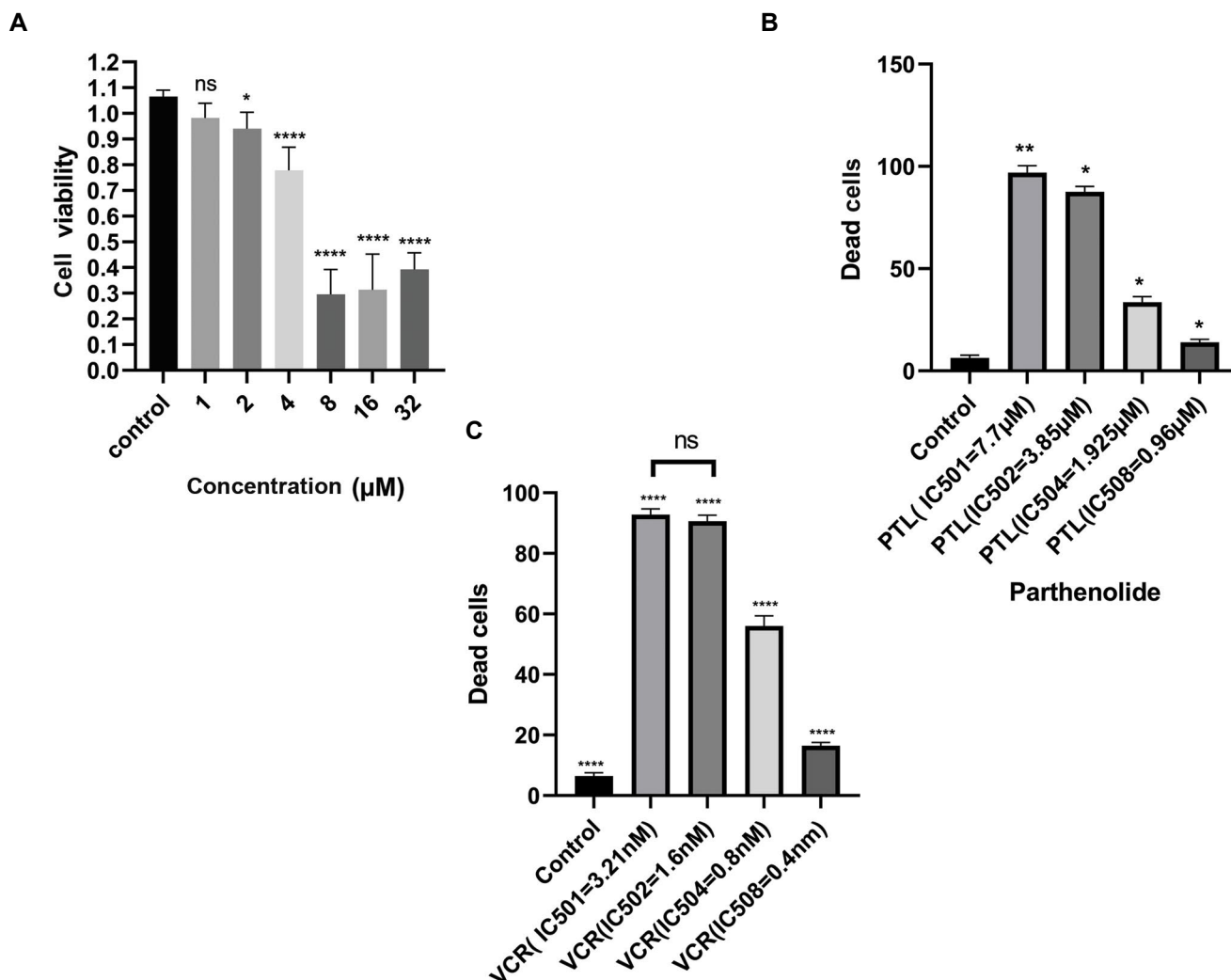


Fig.1: Assessment of cell viability and metabolic activity through MTT and PI assays. **A.** The viability of NALM6 cells exposed to different concentrations of parthenolide after 48 hours (ns; Nonsignificant, *, $P < 0.05$, and ****; $P < 0.0001$). **B.** Flow cytometric analysis of PI staining on NALM6 cells incubated with different concentrations of parthenolide extract after 48 hours (*, $P = 0.028$ and **, $P = 0.0011$). **C.** PI staining on NALM6 cells incubated with different concentrations of vincristine after 48 hours (****; $P < 0.0001$). VCR; Vincristine, PTL; Parthenolide, MTT; (3-(4,5-dimethylthiazol-2-yl)-2,5-diphenyltetrazolium bromide, a tetrazole), and PI; Propidium iodide.

Parthenolide in combination with vincristine promotes apoptosis in NALM6 cells

The Annexin-V-FITC/propidium iodide double staining assay showed that there were 10.73% apoptotic cells in the control group, increasing to 83.2% among the cells treated with the optimal combination of parthenolide (1.925 μ M) and vincristine (1.2 nM) for 48 hours (Fig.2C). In contrast, 50.1 and 58.6% of NALM6 cells were apoptotic when treated for 48 hours with parthenolide or vincristine alone, respectively (Fig.2D). In addition, early apoptotic cells accounted for 15.1, 17.5, and 10.3% of the cells in parthenolide, vincristine, and combination groups, respectively. It was found that 1.925 μ M parthenolide with 1.2 nM vincristine had a robust synergistic inhibitory effect, leaving only 14% living cells after 48 hours of combination therapy (Fig.S1, See Supplementary Online Information at www.celljournal.org).

miR-17-5p, miR-125b-5p, and miR-181b-5p were downregulated in NALM6 cells receiving combination treatment

In the present study, the expression status of these miRNAs in parthenolide-, vincristine-, and combination-treated NALM6 cells was examined by quantitative RT-PCR. The results of RT-PCR analysis showed that different concentrations of parthenolide and vincristine caused variable changes in the expression of miR-17-5p (Fig.3A, B and respectively). Additionally, Figure 3C, D shows that the combined treatment of vincristine and parthenolide led to a decrease in

the expression of miR-17-5p in general. Furthermore, Figure 3E shows that treatment with parthenolide extract caused significant decrease in the expression of miR-125b-5p. However, vincristine did not reduce the expression of miR-125b-5p but rather increased its expression level (Fig.3F). However, when parthenolide was combined with vincristine, it caused a significant decrease in the expression of miR-125b-5p (Fig.3G, H). Also, RT-PCR results for miR-181b-5p showed that both parthenolide and vincristine caused a significant decrease in the expression of this miRNA (Fig.3I, J). Additionally, the combined treatment noticeably reduced the expression level of miR-181b-5p (Fig.3K).

miR-181b-5p, miR-17-5p, and miR-125b-5p predicted to be apoptosis regulators

We constructed the gene network regulated by each miRNA that was involved in apoptosis signals using Cytoscape. Nodes represent genes while edges represent interactions between those entities. The thickness of an edge is used to visually encode the strength or weight of that interaction. RNAhybrid was the second approach which was employed to recognize the regions in 3' UTRs which have the potential to form a thermodynamically favorable duplex with a specific miRNA. RNAhybrid uses minimum free energy (MFE) to evaluate the predicted binding sites for miRNAs. Figure 4 shows that the most frequently targeted sites are those where the MFE ranges with thresholds of -10 kcal/mol and the nucleotide position range is 0-4000 base pairs.

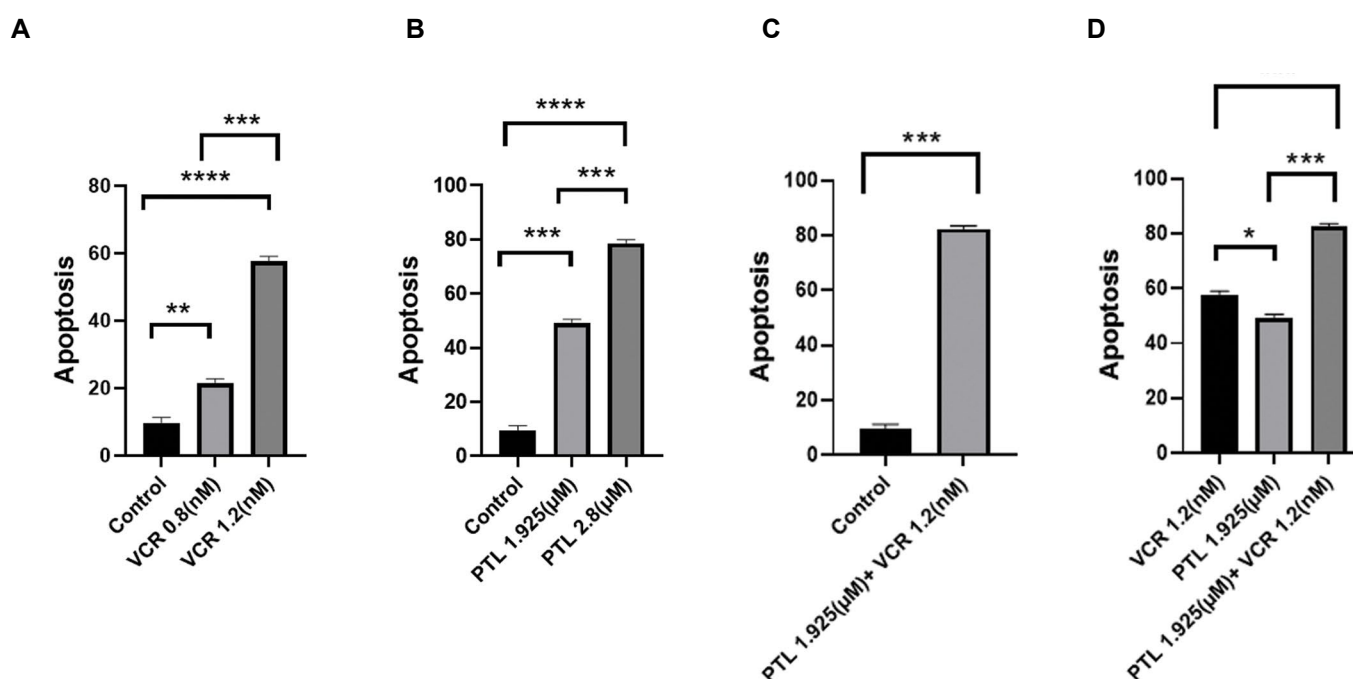


Fig.2: The results of apoptosis following different treatments of NALM6 cell line after 48 hours. **A.** The statistical analysis of the data after treatment with vincristine (**; $P=0.0089$, ***; $P<0.001$, and ****; $P<0.0001$). **B.** Treatment with parthenolide (**; $P<0.001$ and ****; $P<0.0001$). **C.** Combined treatment (**; $P=0.0004$). **D.** The analysis of the combined data compared to separate treatments (*; $P=0.0172$ and ***; $P<0.001$). VCR; Vincristine, and PTL; Parthenolide.

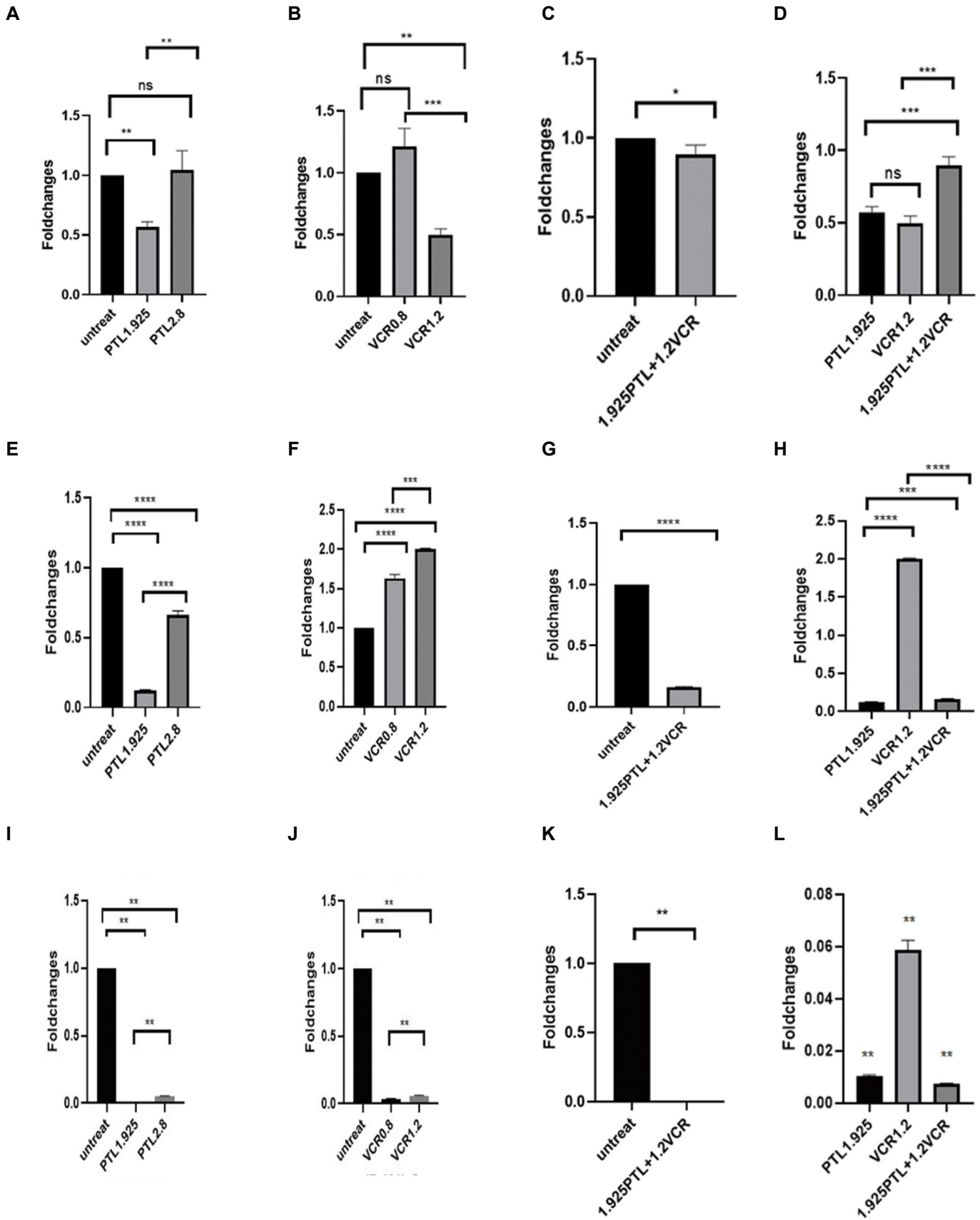


Fig.3: RT-PCR analysis of miRNAs following different treatments for 48 hours. **A.** Alterations in the expression of miR-17-5p following treatment with parthenolide (**; $P < 0.01$). **B.** Vincristine (**; $P = 0.0011$ and ***; $P < 0.0001$). **C.** Combination therapy (*; $P = 0.0363$). **D.** Comparison of combination therapy with separated treatments (***; $P < 0.001$). **E, F.** Show miR-125b-5p expression changes after treatment with parthenolide (****; $P < 0.0001$) and vincristine (***; $P = 0.0002$ and ****; $P < 0.0001$), respectively. **G.** Combination therapy (****; $P < 0.0001$). **H.** Comparison between combination therapy and separated treatments (***; $P = 0.0003$ and ****; $P < 0.0001$). **I.,** miR-181b-5p expression changes following treatment with parthenolide (**; $P < 0.01$), **J.** Vincristine (**; $P < 0.01$). **K.** and combination therapy (**; $P < 0.01$) and **L.** comparison of combination therapy with separated treatments (**; $P < 0.01$). VCR; Vincristine, PTL; Parthenolide, and RT-PCR; Real time -polymerase chain reaction.

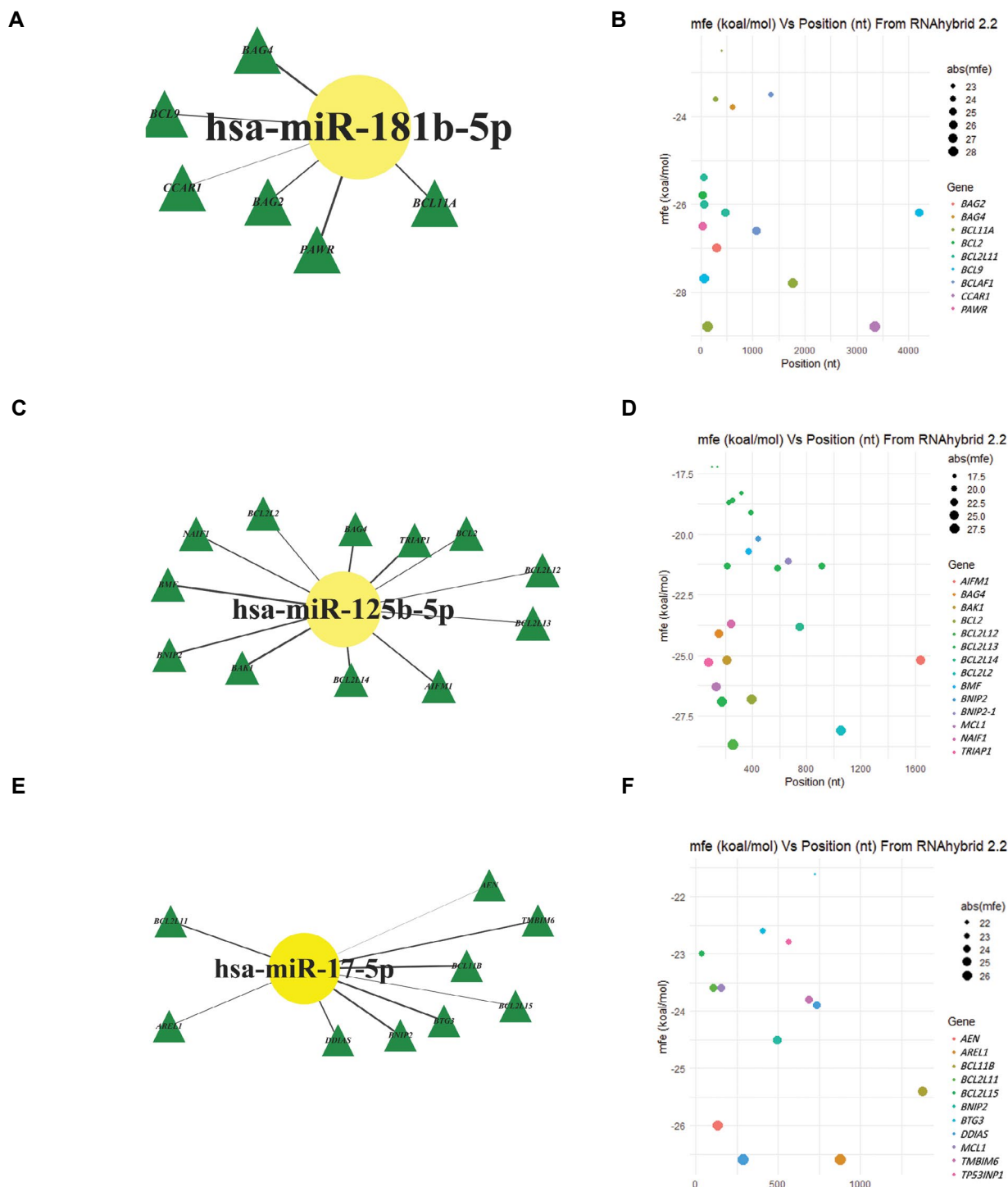


Fig.4: Original Network Analysis using Cytoscape. Given the data of the miRDB dataset, three network analyses of each miRNA were performed with Cytoscape to show that genes regulating apoptosis are targeted by these miRNAs. **A.** miR-181b-5p, **C.** miR-125b-5p, and **E.** miR-17-5p. A thicker edge indicates a stronger interaction between the two nodes it connects. Target sites of human miRNAs on the genes which were analysed with Cytoscape, predicted by RNAhybrid server. **B.** miR-181b-5p, **D.** miR-125b-5p, and **F.** miR-17-5p. There is no direction for edges.

Molecular docking with Auto Dock Vina

Molecular docking is a computational technique that predicts the binding mode and affinity of a small molecule to a target macromolecule. This technique can support the findings of an experiment. Molecular docking is an attractive platform for understanding ligand-miRNA interactions in molecular modeling and rational medication design. This method makes the ligand more flexible and

uses more detailed molecular mechanics to determine the ligand's energy in the setting of a possible active location. AutoDock Vina is an open-source program that performs molecular docking. It uses a scoring function to evaluate the binding affinity of a ligand to target macromolecules. The scoring function is based on the predicted free energy of binding, which is calculated using a grid-based algorithm. The results obtained from molecular docking by AutoDock Vina along with the binding affinity of each

ligand to free miRNAs and mRNAs complexed with the other ligands are shown in Figure 5. The experimental data completely corroborated the results obtained from molecular docking (Fig.5).

Pathways analysis of miRNAs

In this analysis, KEGG pathway enrichment was

performed using the ggplot2 package in R software. The results were then visualized using a bubble plot, where each bubble represents a differential signaling pathway for each miRNA. The Y-axis indicates the pathway name while the X-axis indicates the enriched factor in each pathway. The size and darkness of the bubbles in blue color represent the significance of the pathway (Fig.6).

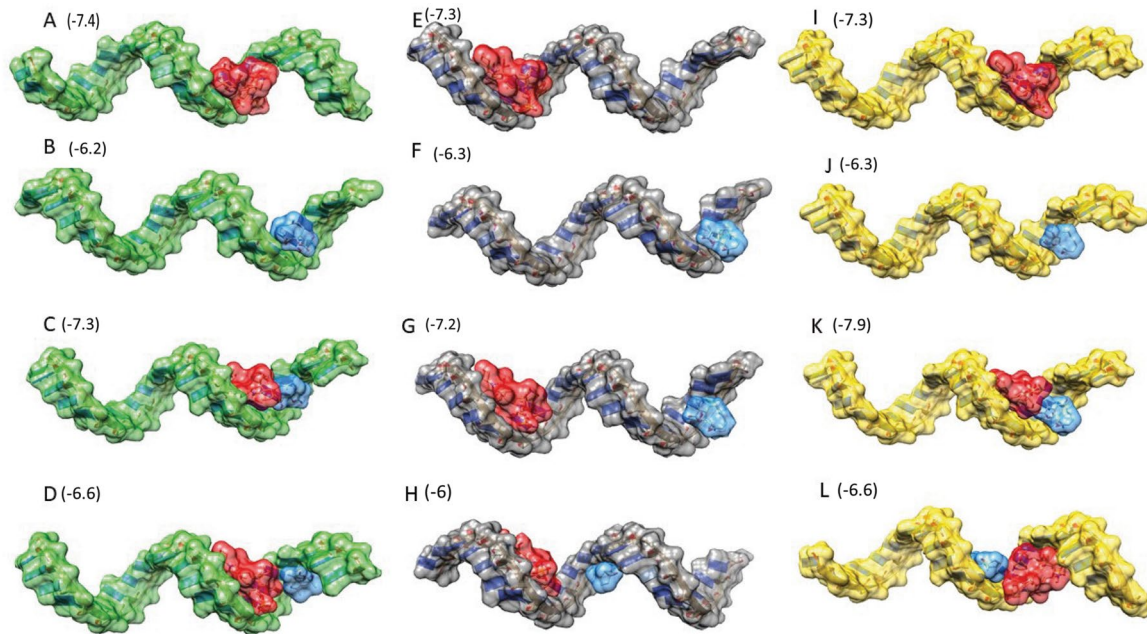


Fig.5: Molecular Docking analysis. The predicted 3D structures of mature miRNAs with vincristine and parthenolide. The green, gray, yellow, red, and blue colors indicate miR-17-5p, miR-125b-5p, miR-181b-5p, vincristine, and parthenolide, respectively. The numbers in the picture represent the binding affinity of each interaction.

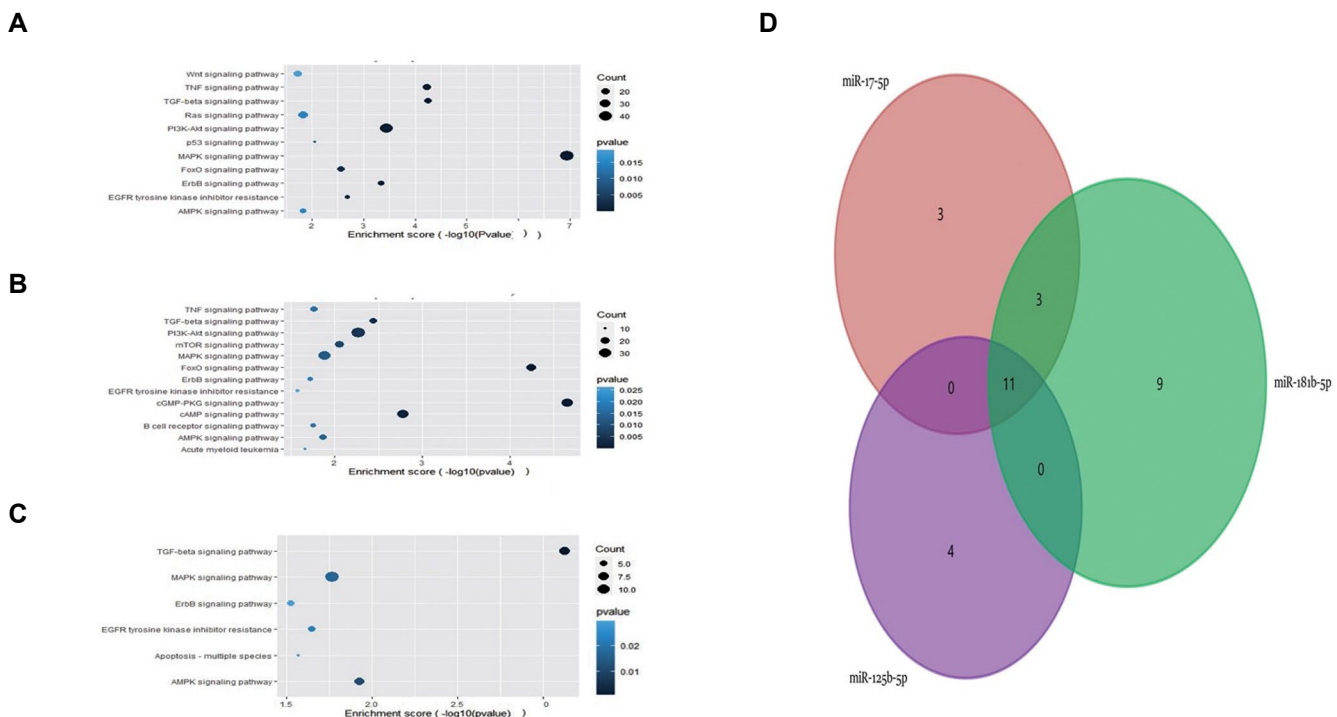


Fig.6: Pathway enrichment analyses of the differentially expressed genes related to each miRNA. Using $P \leq 0.05$ as a threshold. **A.** miR-17-5p, **B.** miR-181b-5p, and **C.** miR-125b-5p. Items showed significant changes. **D.** Venn diagram of 3 miRNAs via pathways.

Discussion

The treatment of ALL is occasionally associated with resistance and there is a need for new treatment strategies. The study investigated the effects of parthenolide and vincristine on the expression of miR-17-5p, miR-181b-5p, and miR-125b-5p, as well as apoptosis in the NALM6 cell line. Our novel findings revealed that the expression of these miRNAs decreased and the rate of apoptosis increased after the treatment. The study also suggested that these miRNAs are negative regulators of apoptosis, and targeting them leads to the inhibition of the PI3K pathway, resulting in increased apoptosis.

Natural compounds have provided a range of alternative drugs for cancer treatment, and one such compound is parthenolide. A study conducted on patients with acute and chronic myelogenous leukemia (AML and CML) showed that parthenolide has low cytotoxicity in normal tissues (17). Additionally, JorgeJ et al. (14) declared that parthenolide could decrease cell viability in various cancer cell lines, including NCI-H929 (Multiple Myeloma), Farage (GCB-DLBCL), Raji (Burkitt Lymphoma), 697, KOPN-8 (B-ALL), CEM, and MOLT-4 (T-ALL). Herein, we assessed the therapeutic potential of parthenolide and its impact on the viability of the NALM6 cell line. Our findings indicated that parthenolide can decrease the metabolic activity and viability of NALM6 cells in a dose-dependent manner, after incubation for 48 hours. Our results are in accordance with Flores-Lopez et al. (18) discovered that parthenolide and DMAPT (a parthenolide analog) have a strong inhibitory effect on CML cells (K562, Meg-01, and KCL-22).

Interestingly, our data suggest that parthenolide has a strong impact on the NALM6 cell line, reducing metabolic activity by 50% within 48 hours at a concentration of approximately 7.7 μM . Moreover, the PI studies indicated decreased cell viability in a dose-dependent manner. A previous study demonstrated that combining paclitaxel with a lethal dose of parthenolide led to a significant increase in cell apoptosis in gastric cancer cells. Similarly, in mice with A549 tumors, parthenolide enhanced the activity of paclitaxel (19). This is in line with our study that utilized flow cytometry to determine if the loss of cell viability was due to apoptosis. We also evaluated the combinational effects of parthenolide and vincristine *in vitro*. The results of Annexing V-FITC/PI double staining showed that the most effective combination which was 1.925 μM parthenolide and 1.2 nM vincristine in NALM6 cells, proved to be more effective than either agent alone. The rate of apoptosis was 1.66- and 1.41-fold higher compared to parthenolide or vincristine alone in NALM6 cells. These findings support those of another study that found parthenolide enhanced the toxicity of arsenic trioxide (ATO) in T-cell leukemia/lymphoma cells *in vitro* (20). Moreover, our study confirmed that parthenolide has a robust anti-apoptotic effect in NALM6 cells whether in combination or alone.

Parthenolide has anticancer effects due to its chemical

structure. It can interact with proteins in cancer cells and disrupt multiple signaling pathways. One key action is inducing apoptosis in cancer cells that is linked to inhibiting NF- κB , a protein complex involved in cancer cell survival, generating reactive oxygen species (ROS), and causing mitochondrial dysfunction. Its natural origin makes it an appealing potential alternative to conventional chemotherapy drugs (21).

Overall, ALL is recognized as a genetic disease. However, the significance of epigenetic changes, particularly alteration of miRNAs, has become more apparent in the development of leukemia (22). Multiple studies have identified numerous miRNAs that exhibit abnormal apoptosis signaling in individuals with ALL (23). Consequently, there is growing interest in exploring the potential benefits of simultaneously targeting apoptosis signaling and modulating miRNAs. MiRNAs such as miR-181b-5p, miR-125b-5p, and miR-17-5p have significant involvement in the regulation of apoptosis, particularly in ALL (10, 23).

Moreover, to further understand how miR-17-5p, miR-125b-5p, and miR-181b-5p affect apoptosis, the target genes of those miRNAs were identified using miRDB and the Cytoscape network. Also, to confirm that these miRNAs are regulators of apoptosis, the genes related to apoptosis were imported to RNAhybrid tool and the potential binding sites for the studied miRNAs on each gene sequence with minimum energy were obtained.

In this study, we conducted quantitative RT-PCR to assess the expression levels of miR-181b-5p, miR-125b-5p, and miR-17-5p in the NALM6 cell line. The results of RT-PCR analysis showed that different concentrations of parthenolide and vincristine caused variable changes in the expression of miR-17-5p. However, the selected concentration of parthenolide (1.925 μM) and vincristine (1.2 nM) used for synergy in the apoptosis section, both caused a significant decrease in the expression level of this miRNA compared to the untreated cells. Additionally, the combined treatment of vincristine and parthenolide led to a decrease in the expression of miR-17-5p in general. Furthermore, treatment with parthenolide extract caused a significant decrease in the expression of miR-125b-5p (8.03-fold lower). While vincristine did not reduce the expression of miR-125b-5p, it increased its expression level. However, when parthenolide was combined with vincristine, which was actually our selected synergy point, it caused a significant decrease in the expression of miR-125b-5p (6.13 and 12.29-fold lower than the untreated and vincristine-treated group, respectively). The RT-PCR results for miR-181b-5p showed that both parthenolide and vincristine caused a significant decrease in the expression of this miRNA.

Additionally, the combined treatment (parthenolide and vincristine) caused a sharp reduction in the expression levels of miR-181b-5p. Moreover, the power of parthenolide in reducing the expression of miR-181b-5p was greater than that of vincristine (95.87-fold and 17-

fold lower, respectively).

While we mentioned these miRNAs are regulators of apoptosis and showed that they have interacted with parthenolide and vincristine, to validate their interaction, molecular docking was performed. Our experimental data of miRNAs is in line with the results of docking analysis. For example, the increase in miR-125b-5p following treatment with vincristine is probably due to the different binding site of the drug for miR-125b-5p, which binds to the 5' end. Likewise, it can be concluded that the decrease in the expression of miR-125b-5p observed when the combination treatment was carried out, was mainly caused by parthenolide and not vincristine.

Pathway enrichment and bioinformatic study for the mentioned miRNAs demonstrated that PI3K signaling was the common significant pathway between miR-17-5p and miR-181b-5p, while transforming growth factor- β (TGF- β) was the most significant pathway for miR-125b-5p and miR-181b-5p. Therefore, it can be concluded that both miR-181b-5p and miR-17-5p target the PI3K pathway by commonly targeting the genes AKT, ERK, and PI3K, while miR-125b-5p and miR-181b-5p target TGF- β which is the upstream pathway of PI3K. Therefore, PI3K is probably the downstream mechanism of these miRNAs that leads to apoptosis. According to the results, it seems that miR-181b-5p, miR-17-5p, and miR-125b-5p can be used as biomarkers for patient follow-up and evaluating response to treatment.

This novel discovery suggests that the combination of parthenolide and vincristine has a synergistic effect on inducing apoptosis in NALM6 cells, potentially through the downregulation of studied miRNAs and their associated pathways. These findings contribute to a deeper understanding of the molecular mechanisms underlying the anti-cancer effects of this combination therapy. However, there are some limitations. Only one cell line was used, and a combination index is lacking. However, the key strengths are demonstrating parthenolides' potent anti-apoptotic effects alone and in combination with vincristine, revealing synergistic induction of apoptosis by miRNAs, and supporting further development of parthenolide as an epigenetic therapy targeting dysregulated miRNAs in B-ALL. Accordingly, the study recommends parthenolide as a novel epigenetic modulator for combination therapy to overcome drug resistance in B-ALL targeting dysregulated miR-125b-5p, miR-17-5p, and miR-181b-5p.

Conclusion

The results of the current research show that the combination of parthenolide and vincristine has a greater capacity to inhibit NALM6 cell viability than either agent alone. The anti-cancer mechanism of the combination appears to involve cell apoptosis. Therefore, parthenolide and vincristine can be considered for combined use as a complementary strategy to treat B-ALL after animal model studies. Hence, our experimental and bioinformatics

investigations demonstrate that combination therapy modulates the expression of mentioned miRNAs, which are drivers of apoptosis. Also, this research suggests miR-17-5p, miR-181b-5p, and miR-125b-5p as therapeutic biomarkers for B-ALL patients with resistance to apoptosis. Further research is warranted to evaluate both agents in more ALL models, elucidate the experimental molecular mechanisms for the PI3K pathway, and assess therapeutic potential *in vivo* before clinical translation.

Acknowledgments

This study was conducted as thesis of Atefeh Bahmei in Hematology and Blood Bank at Shiraz University of Medical Sciences, Shiraz, Iran. We would like to express our gratitude to Shiraz University of Medical Sciences for financially support in conducting this study. We also extend our appreciation to the staff of the Diagnostic Laboratory Sciences and Technology Research Center at the School of Paramedical Sciences, Shiraz University of Medical Sciences, Shiraz, Iran. There is no conflict of interest in this study.

Authors' Contributions

G.T.; Contributed to conception, Design, and Responsible for overall supervision. A.B., S.N.; Contributed to all experimental work, Data acquisition, and Statistical analysis. M.Y.-M.; Statistical analysis and Performed the analysis of molecular docking. A.B., A.E.; Contributed to bioinformatics analysis and R software analysis. R.R.; Supervised the statistical analysis as well as the interpretation of data. All authors read and approved the final manuscript.

References

1. Inaba H, Pui CH. Advances in the diagnosis and treatment of pediatric acute lymphoblastic leukemia. *J Clin Med*. 2021; 10(9): 1926.
2. Bhojwani D, Yang JJ, Pui CH. Biology of childhood acute lymphoblastic leukemia. *Pediatr Clin North Am*. 2015; 62(1): 47-60.
3. Sheykhasan M, Manoochehri H, Dama P. Use of CAR T-cell for acute lymphoblastic leukemia (ALL) treatment: a review study. *Cancer Gene Ther*. 2022; 29(8-9): 1080-1096.
4. Pui CH. Precision medicine in acute lymphoblastic leukemia. *Front Med*. 2020; 14(6): 689-700.
5. ATCC. NALM6, clone G5. available from <https://www.atcc.org/products/crl-3273> (16 Oct 2023)
6. O'Brien J, Hayder H, Zayed Y, Peng C. Overview of MicroRNA biogenesis, mechanisms of actions, and circulation. *Front Endocrinol (Lausanne)*. 2018; 9: 402.
7. Ranganathan K, Sivasankar V. MicroRNAs - biology and clinical applications. *J Oral Maxillofac Pathol*. 2014; 18(2): 229-234.
8. Souza OF, Popi AF. Role of microRNAs in B-cell compartment: development, proliferation and hematological diseases. *Biomedicines*. 2022; 10(8): 2004.
9. Lv M, Zhu S, Peng H, Cheng Z, Zhang G, Wang Z. B-cell acute lymphoblastic leukemia-related microRNAs: uncovering their diverse and special roles. *Am J Cancer Res*. 2021; 11(4): 1104-1120.
10. Vafadar A, Mokaram P, Erfani M, Yousefi Z, Farhadi A, Elham Shirazi T, et al. The effect of decitabine on the expression and methylation of the PPP1CA, BTG2, and PTEN in association with changes in miR-125b, miR-17, and miR-181b in NALM6 cell line. *J Cell Biochem*. 2019; 120(8): 13156-13167.
11. Bousquet M, Harris MH, Zhou B, Lodish HF. MicroRNA miR-125b causes leukemia. *Proc Natl Acad Sci U S A*. 2010; 107(50): 21558-21563.
12. Kari S, Subramanian K, Altomonte IA, Murugesan A, Yli-Harja

- O, Kandhavelu M. Programmed cell death detection methods: a systematic review and a categorical comparison. *Apoptosis*. 2022; 27(7-8): 482-508.
13. Ghorbani-Abdi-Saedabad A, Hanafi-Bojd MY, Parsamanesh N, Tayarani-Najaran Z, Mollaei H, Hoshyar R. Anticancer and apoptotic activities of parthenolide in combination with epirubicin in mda-mb-468 breast cancer cells. *Mol Biol Rep*. 2020; 47(8): 5807-5815.
 14. Jorge J, Neves J, Alves R, Geraldes C, Gonçalves AC, Sarmiento-Ribeiro AB. Parthenolide Induces ROS-mediated apoptosis in lymphoid malignancies. *Int J Mol Sci*. 2023; 24(11): 9167.
 15. Trott O, Olson AJ. AutoDock Vina: improving the speed and accuracy of docking with a new scoring function, efficient optimization, and multithreading. *J Comput Chem*. 2010; 31(2): 455-461.
 16. Pettersen EF, Goddard TD, Huang CC, Couch GS, Greenblatt DM, Meng EC, et al. UCSF Chimera--a visualization system for exploratory research and analysis. *J Comput Chem*. 2004; 25(13): 1605-1612.
 17. Guzman ML, Rossi RM, Karnischky L, Li X, Peterson DR, Howard DS, et al. The sesquiterpene lactone parthenolide induces apoptosis of human acute myelogenous leukemia stem and progenitor cells. *Blood*. 2005; 105(11): 4163-419.
 18. Flores-Lopez G, Moreno-Lorenzana D, Ayala-Sanchez M, Aviles-Vazquez S, Torres-Martinez H, Crooks PA, et al. Parthenolide and DMAPT induce cell death in primitive CML cells through reactive oxygen species. *J Cell Mol Med*. 2018; 22(10): 4899-4912.
 19. Sztiller-Sikorska M, Czyz M. Parthenolide as cooperating agent for anti-cancer treatment of various malignancies. *Pharmaceuticals (Basel)*. 2020; 13(8): 194.
 20. Kouhpaikar H, Sadeghian MH, Rafatpanah H, Kazemi M, Iranshahi M, Delbari Z, et al. Synergy between parthenolide and arsenic trioxide in adult T-cell leukemia/lymphoma cells in vitro. *Iran J Basic Med Sci*. 2020; 23(5): 616-622.
 21. Freund RRA, Gobrecht P, Fischer D, Arndt HD. Advances in chemistry and bioactivity of parthenolide. *Nat Prod Rep*. 2020; 37(4): 541-565.
 22. Ranjbar R, Karimian A, Aghaie Fard A, Tourani M, Majidinia M, Jadidi-Niaragh F, et al. The importance of miRNAs and epigenetics in acute lymphoblastic leukemia prognosis. *J Cell Physiol*. 2019; 234(4): 3216-3230.
 23. Lv M, Zhu S, Peng H, Cheng Z, Zhang G, Wang Z. B-cell acute lymphoblastic leukemia-related microRNAs: uncovering their diverse and special roles. *Am J Cancer Res*. 2021; 11(4): 1104-1120.
-